ELSEVIER

Thin Solid Films 369 (2000) 405–408

thin solid films

www.elsevier.com/locate/tsf

Growth and characterization of $^{70}Ge_n/^{74}Ge_n$ isotope superlattices

K. Morita[a,*], K.M. Itoh[a, b], J. Muto[a], K. Mizoguchi[c], N. Usami[d], Y. Shiraki[d], E.E. Haller[e]

[a]*Department of Applied Physics and Physico-Informatics, Keio University, Yokohama, 223-8522 Japan*
[b]*PRESTO-JST, Yokohama, 223-8522 Japan*
[c]*Department of Applied Physics, Osaka City University, Osaka, 558-8585 Japan*
[d]*RCAST, Univ. of Tokyo, Tokyo, 153-8904 Japan*
[e]*UC Berkeley and Lawrence Berkeley National Labs, Berkeley, CA 94720, USA*

Abstract

We report on the molecular beam epitaxial (MBE) growth of $^{70}Ge_n/^{74}Ge_n$ isotope superlattices composed of alternating layers of the stable isotopes ^{70}Ge and ^{74}Ge. Samples prepared in this work have atomic layers $n = 4$, 8, 16, and 32. All superlattices are p-type having a net-impurity concentration of $\sim 10^{16}\,cm^{-3}$. Zone-folding of optical phonons due to the mass periodicity in the growth direction has been observed clearly for all samples using high resolution Raman spectroscopy. The corresponding phonon mode of each Raman peak has been indexed according to theoretical calculations using the linear-chain model and the planar bond-charge model. The frequency of the Raman peaks found by the experiment agree very well with those of the phonon modes calculated for each superlattice structure. A detailed analysis of the Raman spectra concludes that the degree of interface mixing between ^{70}Ge and ^{74}Ge layers for our typical growth condition is less than two monolayers.

Keywords: Isotope superlattices; Molecular beam epitaxy; Raman scattering; LO phonons; Linear-chain model; Interface mixing

1. Introduction

The development of the molecular beam epitaxy has lead to the successful fabrication of semiconductor superlattices that are composed of alternating thin layers of different chemical constituents, e.g. GaAs/GaAlAs, GaN/GaAlN, etc. In these conventional structures, the periodicity in the alternating layers in the growth direction lead to zone-folding of both the electronic band structures and the phonon dispersion curves. In this work we have grown $^{70}Ge_n/^{74}Ge_n$ isotope superlattices composed of alternating layers of the stable isotopes ^{70}Ge and ^{74}Ge. n denotes the thickness of the each isotope layer in units of atomic monolayers. These superlattices are unique in the sense that the alternating layers are composed of the same chemical elements but with different atomic masses, i.e. while the electronic band structure is practically the same as that of bulk Ge, the phonon dispersion curve is zone-folded due to the mass periodicity in the direction of the growth. Therefore the isotope superlattices allow us to probe exclusively the nature of phonons in low dimensional structures.

In this work, we have characterized the isotope superlattices using Raman spectroscopy. Raman scattering is believed to be the best method to characterize the short period isotope superlattices, since for example X-ray diffraction analysis can be used only for superlattices composed of different chemical constituents. The depth resolution of the secondary mass ion spectroscopy (SIMS) is not sufficient to characterize the isotope superlattices of the layer thickness of the order of a hundred angstroms or less. Excellent agreement between experimentally measured Raman phonon peak positions and theoretically calculated phonon frequencies for each isotope superlattice will be reported. Pioneering work of this kind has been performed recently by Haller, Cardona, and their co-workers [1–3].

2. Phonons in $^{70}Ge_n/^{74}Ge_n$ isotope SLs

We shall discuss phonons in $^{70}Ge_n/^{74}Ge_n$ isotope superlattices using the $^{70}Ge_{16}/^{74}Ge_{16}$ superlattice as an example. The phonon dispersion of a $^{70}Ge_{16}/^{74}Ge_{16}$ isotope superlattice in the $\langle 100 \rangle$ growth direction (solid curve) and that of bulk ^{nat}Ge (dashed curve) are shown in Fig. 1. Only longitudinal branches are shown for the isotope superlattice. The dispersion of the superlattice is zone-folded and its Brillouin zone is 16 times smaller than that of bulk Ge. In the back scattering Raman geometry, all transverse phonons are Raman forbidden by the symmetry in the $\langle 100 \rangle$ direction

* Corresponding author.

0040-6090/00/$ - see front matter
PII: S0040-6090(00)00901-9

of the superlattice. Therefore only Γ-point LO phonons having A_g symmetry are Raman active [2].

In order to obtain phonon frequencies and vibrational amplitudes of Γ-point LO phonons in $^{70}Ge_n/^{74}Ge_n$ isotope superlattices, we have performed calculations based on the linear-chain model [4]. In this model, atomic planes of ^{74}Ge layers and ^{70}Ge layers are connected by simple springs. Only the interaction between the nearest neighboring planes has been taken into account in our calculation. Because $^{70}Ge_n/^{74}Ge_n$ isotope superlattices are composed of one type of chemical elements, we assume that the force constants of the springs between ^{70}Ge–^{70}Ge planes, ^{70}Ge–^{74}Ge planes and ^{74}Ge–^{74}Ge planes are the same, and were determined by the peak position of the bulk ^{70}Ge LO phonon. The calculational results of Γ-point LO phonon frequencies and vibrational amplitudes are shown for the $^{70}Ge_{16}/^{74}Ge_{16}$ isotope superlattice in Fig. 2. Raman active phonons having A_g symmetry are marked in Fig. 2. The two confined phonon modes labeled $LO_1(^{70}Ge)$ and $LO_1(^{74}Ge)$ have the strongest vibrational amplitudes.

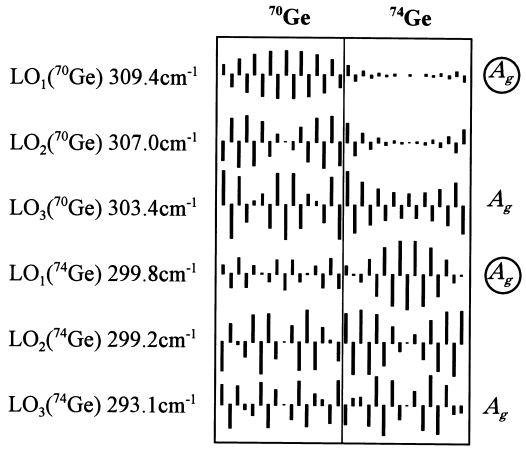

Fig. 2. Vibrational amplitude of longitudinal optical (LO) phonons in each isotopic layer determined by the linear-chain model. Frequencies of modes are shown on the left. Raman active phonons are labeled A_g. Two encircled $LO_1(^{70}Ge)$ and $LO_1(^{74}Ge)$ phonons corresponds to two major peaks in Raman spectra.

3. Experiment

We have grown four $^{70}Ge_n/^{74}Ge_n$ isotope superlattices with $n = 4$, 8, 16, and 32 by the solid-source MBE technique. The sources of ^{70}Ge and ^{74}Ge we used were isotropically enriched to 96.3 and 96.8%, respectively. The superlattices were grown on the top of a 200Å thick ^{70}Ge buffer layer along the ⟨100⟩ direction. The temperature of the substrate during the growth was kept at 350°C. The number of periods and total thickness of each sample are shown in Table 1. All superlattices are p-type having a net-impurity concentration of $\sim 10^{16}$ cm^{-3}. Using variable temperature Hall measurements, the majority impurity was found to be boron. High resolution (0.3 cm^{-1}) Raman spectra of the four SLs were recorded in back scattering geometry at $T = 10$ K using the Ar^+ 514 nm-line.

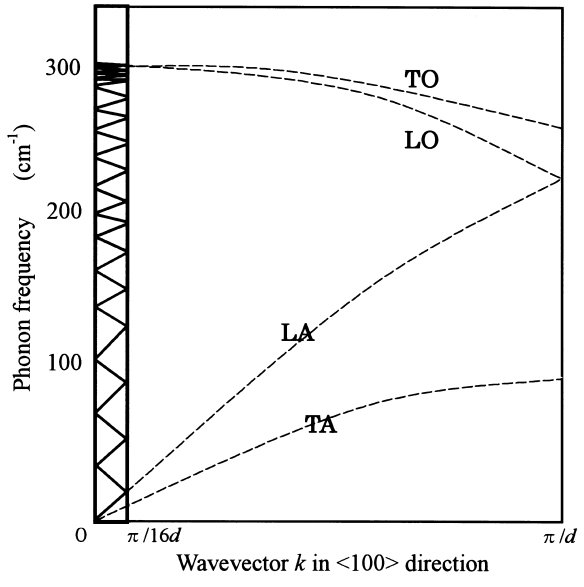

Fig. 1. Phonon dispersion of the $^{70}Ge_{16}/^{74}Ge_{16}$ isotope superlattice (solid curve) and that of bulk Ge (dashed curve).

4. Result and discussion

The measured Raman spectra of the $n = 4$, 8, 16 and 32 $^{70}Ge_n/^{74}Ge_n$ isotope superlattices are shown in Fig. 3. At the top of this figure, the positions of bulk ^{70}Ge and bulk ^{74}Ge LO phonon peaks are indicated by arrows. Two major phonon peaks due to $LO_1(^{70}Ge)$ and $LO_1(^{74}Ge)$ phonons are observed clearly in the $n = 8$, 16 and 32 samples. We can also find a weak $LO_1(^{74}Ge)$ phonon peak near 290 cm^{-1} in the $n = 4$ sample when magnified. The $LO_1(^{70}Ge)$ phonon peak position shifts to higher frequency and approaches the frequency of the bulk ^{70}Ge LO-phonon as n is increased. On the other hand the $LO_1(^{74}Ge)$ phonon peak position stays at the same frequency, but grows in intensity when n is increased. Further analysis has shown that it is necessary to combine more than two Lorentzian peaks in order to reproduce our Raman spectra. Fig. 4 shows the Lorentzian deconvolution of the Raman spectra for the $n = 8$, 16, and 32 samples. The spectra of the $n = 8$ samples are composed of three phonon peaks; two major ones corresponding to $LO_1(^{70}Ge)$ and $LO_1(^{74}Ge)$, and one small peak in between.

Table 1
Isotopic layer thickness n, numbers of periods, and total thickness of superlattices prepared in this work

N	Periods	Total thickness (Å)
4	35	400
8	18	400
16	13	600
32	6	600

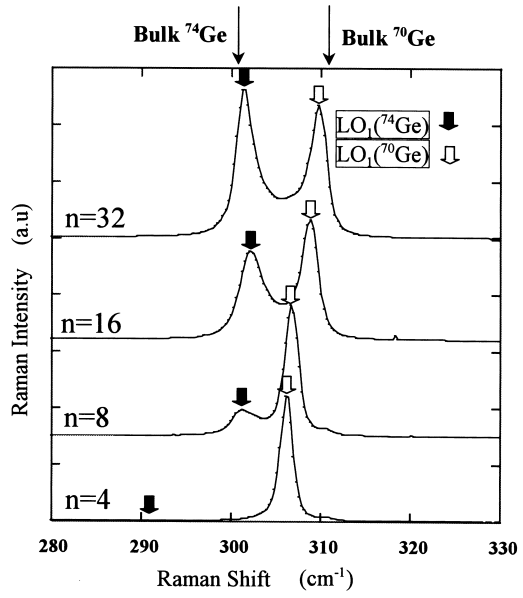

Fig. 3. The Raman spectra of $^{70}Ge_n/^{74}Ge_n$ isotope superlattices.

The spectrum of $n = 32$ sample is composed of five peaks; two major ones and three small peaks in between. The middle peak in the $n = 16$ samples has been assigned to the LO$_3$(^{70}Ge) phonon while the three small middle peaks in the $n = 32$ sample have been assigned to LO$_3$(^{70}Ge), LO$_5$(^{70}Ge), and LO$_7$(^{70}Ge). Fig. 5a shows the direct comparison of the phonon peak positions found from the experiment (filled circles) and from calculations using the linear-chain model (solid curve). The agreement between the experimental and theoretical results is good except for the one detail; for the $n = 32$ sample, five phonon peaks have been observed in the measured spectra while only four Raman active modes are predicted by the linear-chain model calculation. Fig. 5b is the same figure as Fig. 5a but with theoretical curves due to the planar bond-charge model performed by Spitzer et al. [1,5]. In this case theory predicts five Raman phonon peaks for $n = 32$ samples in accordance with our experimental observation and the overall agreement of the phonon frequencies between experiment and calculation is excellent. Since the planar bond-charge model can be regarded as a higher order calculation of the linear-chain model, it is understandable that our data agree better with the results of the planar bond-charge model than that of the linear-chain model [5].

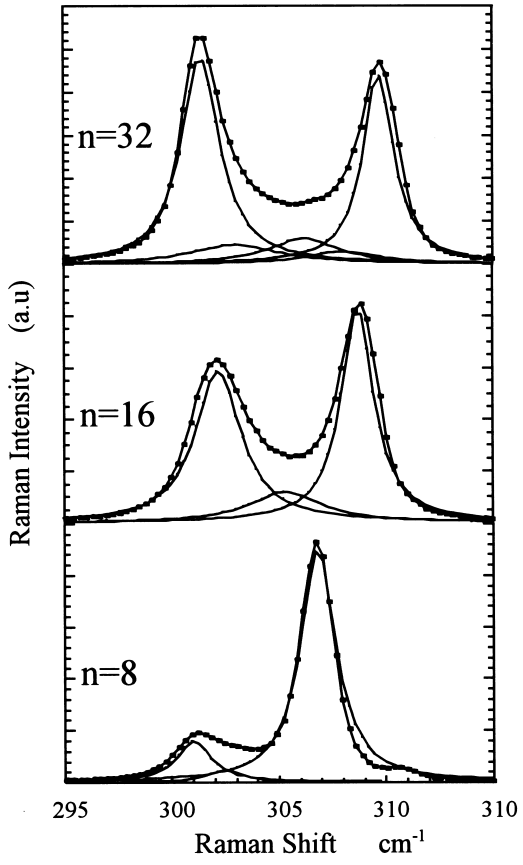

Fig. 4. The result of Lorentzian fits for the $n = 8$, 16, and 32 $^{70}Ge_n/^{74}Ge_n$ samples. Experimental Raman spectra (doted curves) and deconvoluted Lorentzian peaks (solid curves) are shown.

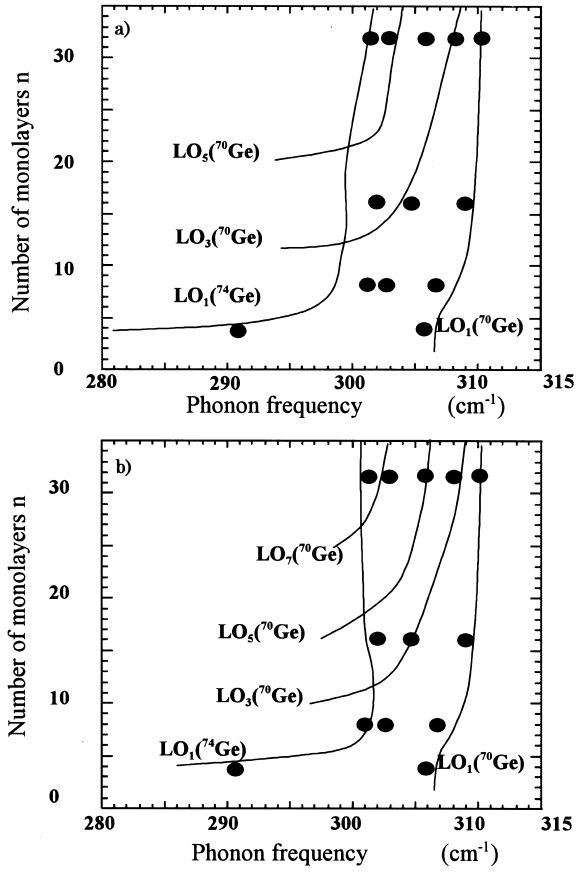

Fig. 5. Direct comparison of the LO phonon frequencies determined by Raman experiments (filled circles) and by calculations (solid curves). Two different models have been employed for the theoretical calculations: (a) linear-chain model and (b) planar bond-charge model. The calculated results shown in (b) have been adopted from Ref. [1].

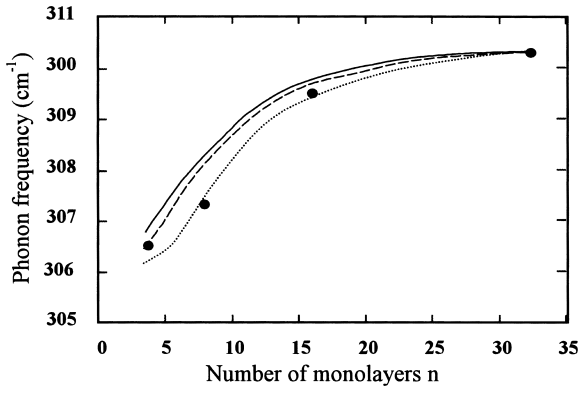

Fig. 6. Experimental results (filled circles) along with calculated results of $LO_1(^{70}Ge)$ phonon frequencies as a function of n. The solid line indicates the calculated results of ideal superlattice. The dashed and dotted lines are calculations considering the intermixing of 1 and 2 monolayers, respectively.

It is also possible to estimate the degree of interface mixing between ^{70}Ge and ^{74}Ge layers for our growth condition by comparing the observed positions of the phonon peaks and the prediction due to the linear-chain model. Fig. 6 shows the comparison of the observed peak position of the $LO_1(^{70}Ge)$ phonons with the results of calculation when no interface mixing was present (solid curve), interface mixing of one monolayer is introduced (dashed curve), and interface mixing of two monolayers is assumed (dotted curve). The $LO_1(^{70}Ge)$ phonon is the appropriate mode for this kind of evaluation since it does not anticross with any other modes. In the calculation we used the model in which the intermixing layer is a 50% alloy of ^{70}Ge and ^{74}Ge and assume that the atomic mass of intermixed layer is the average mass of ^{70}Ge and ^{74}Ge. Taking into account the effect of isotopic disorder at the interfaces, all the calculated results were lowered by 0.6 cm^{-1} [1,3,6]. The result shown in Fig. 6 indicates that the degree of the interface mixing is at most two monolayers.

5. Conclusions

We have successfully grown isotope superlattices of $^{70}Ge_n/^{74}Ge_n$ having $n = 4$, 8, 16, and 32. The phonon peak positions of each sample revealed by Raman spectroscopy agree very well with the prediction of the theoretical calculation. This guarantees the high quality of the isotope superlattices we have fabricated in this work. The degree of interface mixing during our growth condition was found to be less than 2 monolayers.

Acknowledgements

We wish to thank M. Nakajima for the fruitful discussion. The work at Keio is supported in part by a Grant-in-Aid for Scientific Research on the Priority Area ‘Spin Controlled Semiconductor Nanostructures’ from the Ministry of Education, Science, Sports, and Culture. The work at Berkeley was supported in part by the Director, Office of Energy Research, Office of Basic Energy Science, Materials Science Division of the U.S. Department of Energy under Contract No. DE-AC03-76SF00098 and in part by U.S. NSF Grant No. DMR-9732707.

References

[1] J. Spitzer, T. Ruf, M. Cardona, et al., Phys. Rev. Lett. 72 (1994) 1565.
[2] H.D. Fuchs, et al., Superlattices and Microstructure 13 (1993) 447.
[3] T. Ruf, Phonon Raman Scattering in Semiconductors, Quantum Wells and Superlattices, Springer, Heidelberg, 1997, p. 33.
[4] P.Y. Yu, M. Cardona, Fundamentals of Semiconductors, 2nd ed., Springer, Heidelberg, 1998, p. 482.
[5] P. Molinàs-Mata, M. Cardona, Phys. Rev. B 43 (1991) 9799.
[6] P. Etchegoin, H. Fuchs, J. Weber, et al., Phys. Rev. B 48 (1993) 12661.